NUMERICAL SIMULATION OF SELF-FOCUSING OF AN ARRAY ON AN INTERIOR CRACK

Ming Zhang and J. D. Achenbach

Center for Quality Engineering and Failure Prevention
Northwestern University
Evanston, IL 60208

INTRODUCTION

Small cracks inside a solid are difficult to detect using a conventional ultrasonic focused transducer because its focal point and radiation direction are fixed. Using a self-focusing array can enhance the ability of crack detection and characterization because the beam steers itself inside a specimen and focuses the ultrasound on the crack, thereby increasing the ultrasonic signal/noise ratio.

Self-focusing of an array has been achieved by two different approaches: time-reversal processing [1] and adaptive time-delay focusing [2]. In the first technique, beam focusing is achieved with a time-reversal mirror consisting of an array of transducers. The incident acoustic wave is scattered by a target in a solid medium. The scattered wave is sampled, time-reversed and then re-emitted. The re-emitted acoustic wave will focus on the target. The second method of self-focusing consists of four steps as shown in Fig. 1. The first step is to excite the center element of the transducer array to send out a signal. The signal will be scattered by the crack and all elements will receive the scattered signal. From the received signals, the time of flight from the crack to each element can be determined in step 2. In step 3, all elements are excited to send off signals but with the time delays determined in step 2. The transducer which received the signal last in step 2 will be activated first in step 3 in order that all signals will arrive at the crack at the same time. Thus sonification focusing is achieved in this step. The signal backscattered from the crack will again arrive at the elements at different times. In step 4, the signals are aligned to the earliest arrival before summation for reception focusing.

Beam steering and properties of transducer arrays have been studied quantitatively both for a linear transducer array [3] and for a two-dimensional transducer array [4]. The results have been employed in the design of transducer arrays for NDT and medical imaging.

The purpose of this paper is to develop a model that can predict the results of self-focusing of an array on an interior crack. The ray tracing method is used to obtain the wave field incident on a crack in an immersed specimen. The scattering coefficient of a flat crack is calculated by using a reciprocity relationship and the crack opening volume. Numerical results of the scattered fields for various configurations are presented.

MODELING OF SELF-FOCUSING

The measurement model for the self-focusing array is based on elastodynamic ray

Review of Progress in Quantitative Nondestructive Evaluation, Vol. 17
Edited by D.O. Thompson and D.E. Chimenti,, Plenum Press, New York, 1998

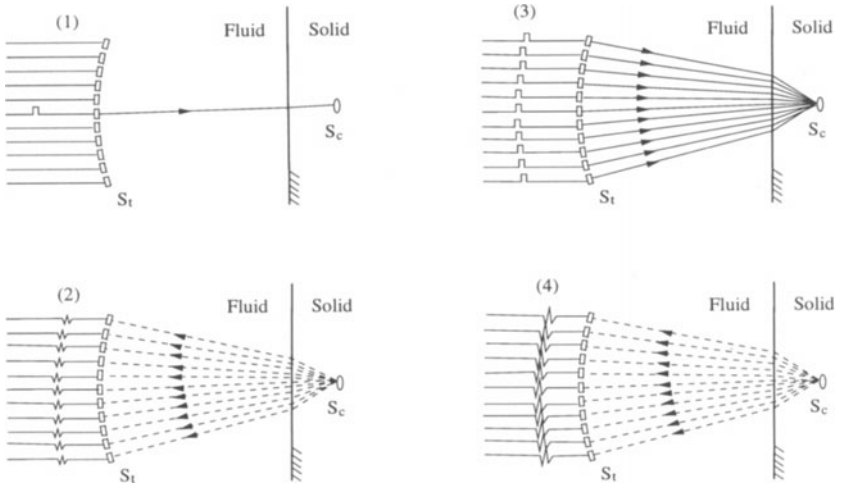

Figure 1: Self-focusing array using time delay method.

theory and a reciprocity relationship. Ray theory is used to trace the wave fields emitted by the transducers and the wave propagation through the water-solid interface to the crack. The reciprocity relationship is employed to obtain the scattering coefficient through the calculation of the crack opening volume. The crack is assumed to be small and sufficiently far from the transducer. The wave fronts are assumed to be nearly planar over the crack surface.

Ray Tracing of the Wave Field Incident on the Crack

Figure 2 shows the pressure field of a circular transducer. The near field is complicated. In the far field, the beam spreading of the pressure field of the transducer can be approximated by a Gaussian distribution,

$$p^f(r,\theta) = \frac{P_0 r_0}{r} e^{-C\theta^2} \tag{1}$$

where P_0 is the pressure at the reference point r_0, C is a beam spreading constant, and where at

$$\theta = \sin^{-1}(0.7\frac{\lambda_w}{D}) \tag{2}$$

the pressure amplitude has decreased by 6dB relative to the pressure on the axis [5]. Here λ_w is the wave length in water and D is the diameter of the transducer. The wave fields are assumed to be time harmonic and the term $e^{-i\omega t}$ has been suppressed. The power of the transmitted wave field is

$$P_t = -\frac{1}{2} i\omega \int_{S_t} p^f u_i^f n_i dS$$

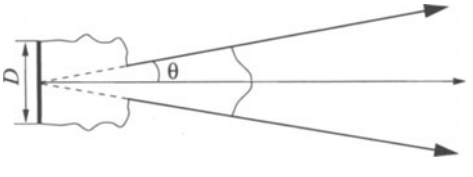

Figure 2. Divergence of the pressure field from a circular transducer.

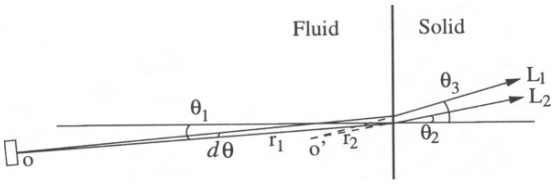

Figure 3. Ray tracing at a fluid-solid interface.

where u_f and P_f define the wave field excited by the transducer and S_t is the area of the transducer.

The specimen immersed in water is assumed to consist of isotropic, homogeneous and linearly elastic material. The interface conditions along the water-solid interface are that the normal components of the displacement and the traction are continuous and the shear traction vanishes:

$$u_n(x) = u_n^f(x), \qquad t_n(x) = -p^f(x), \qquad t_s(x) = 0. \tag{3}$$

The reflection and transmission of a single ray is equivalent to the reflection and transmission of a plane wave. Since the incident wave angles are small, the array elements will receive only a small amount of transverse wave scattering. In the following numerical calculations, only scattering of the longitudinal wave is considered. Let $T_L(\theta_{in}, \kappa, \alpha)$ be the displacement transmission coefficient of a plane L wave incident on a solid from water, where κ is the ratio of the sound speeds ($\kappa = c_l/c_w$) and α is the ratio of the acoustic impedances ($\alpha = z_l/z_w$). T_L can be calculated from the interface conditions. Figure 3 shows the transmission of two neighboring rays. The two rays in the solid appear to come from an imaginary source, where r_2 is approximately equal to r_1/κ. Then the displacement amplitude in the solid may be written as

$$A_L(r) = T_L \cdot u_f(x_{fs}) \cdot \frac{r_2}{r} \tag{4}$$

where $u_f(x_{fs})$ is the displacement field at the fluid side of the interface.

The wave fronts are assumed to be planar over the crack surface. The plane harmonic wave displacement field

$$u_i(x_i) = d_i A_L(r_c) e^{ikx_i \cdot p_i} \tag{5}$$

where d_i and p_i are the components of the displacement and the propagation vectors respectively, $A_L(r_c)$ is the displacement amplitude at the crack. The stress field can be calculated through Hooke's law.

$$\tau_{ij} = \delta_{ij}\lambda u_{l,l} + \mu(u_{i,j} + u_{j,i}) \tag{6}$$

Only the effect of the normal stress τ_{33} is taken into account.

The Scattering Coefficient of a Crack in an Immersed Specimen

Auld [6] and Kino [7] derived a reciprocity relation for the elastic wave scattered by a flaw. Thompson [8] has further applied this relation to ultrasonic scattering measurements through liquid-solid interfaces. In Ref.[8], the relationship between the scattering coefficient of a flaw and the far field scattering amplitudes in the unbounded medium is considered and comparisons between the theoretical and experimental scattering amplitudes have been shown. The theoretical scattering amplitudes were obtained from numerical calculations according to various incident and scattering conditions. In the present work, the reciprocity relation has been employed along with the crack opening volume to calculate the scattering coefficient.

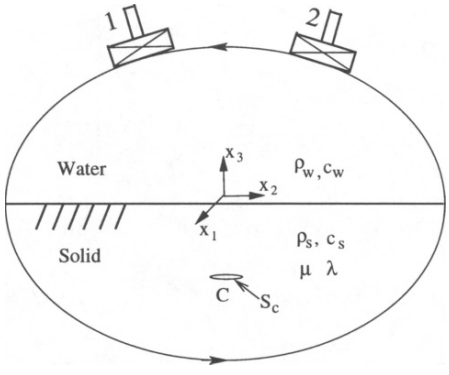

Figure 4. System for calculating the scattering coefficient from a crack.

Figure 4 presents the geometry of a system for calculating the scattering coefficient for a crack using a reciprocity relation. It is assumed that two identical transducers are placed in the fluid and used in a pitch-catch (pulse-echo is a special case) measurement of the scattering from a flat crack. Consider two states: (a) The system is excited by an incident wave carrying unit power from transducer 1, while transducer 2 is receiving. The flaw is *present* in the system. (b) The system is excited by an incident wave carrying unit power from transducer 2, while transducer 1 is the receiver. The flaw is *absent* in the system. The scattering coefficient $S_{21}(\omega)$ is defined as the ratio of the displacement amplitude received by the transducer 2 to the displacement amplitude transmitted from the transducer 1. According to the reciprocity relationship of Ref.[7], the scattering coefficient is

$$S_{21}(\omega) = \frac{1}{4} i\omega \int_{S_c} (u_i^a \cdot \tau_{ij}^b - u_i^b \cdot \tau_{ij}^a) \cdot n_j dS \tag{7}$$

where S_c is the surface of the flaw, n_j is an inward normal to the surface, u_i^a, τ_{ij}^a are the displacement and stress field in state (a) and u_i^b, τ_{ij}^b are the fields produced in state (b). The displacement fields when the flaw is illuminated by transducer '1' can be written as

$$u_i^a(x_i) = u_i^{in}(x_i) + u_i^{sc}(x_i), \qquad x_i \in V \tag{8}$$

The incident field is assumed to be a planar and continuous wave over the flaw. So for a flat crack with faces S_F^+ and S_F^- and located in the x_1x_2-plane

$$\Delta u_i^a = \Delta u_i^{sc}, \qquad \tau_{ij}^a \cdot n_j = 0 \tag{9}$$

where Δu_i^{sc} is the crack opening displacement and the traction free boundary condition at the crack surface is applied. It follows that the scattering coefficient can be written as

$$S_{21}(\omega) = \frac{1}{4} i\omega \int_{S_c^+} \tau_{3i}^b \Delta u_i^{sc} dS \tag{10}$$

Variation of τ_{3i}^b over the faces of the crack is neglected. Only taking into account τ_{33} on the crack faces, the scattering coefficient equation can be further simplified to

$$S_{21}(\omega) = \frac{1}{4} i\omega \tau_{33}^b \int_{S_c^+} \Delta u_3^{sc} dS = \frac{1}{4} i\omega \tau_{33}^b V_3$$

where V_3 is the crack opening volume, and variation of τ_{33} over S_c^+ has been neglected.

The crack opening volume is defined as the integration of the crack opening displacement over the area of the crack

$$V_3 = \int_{s_c} \Delta u_3 dS. \tag{11}$$

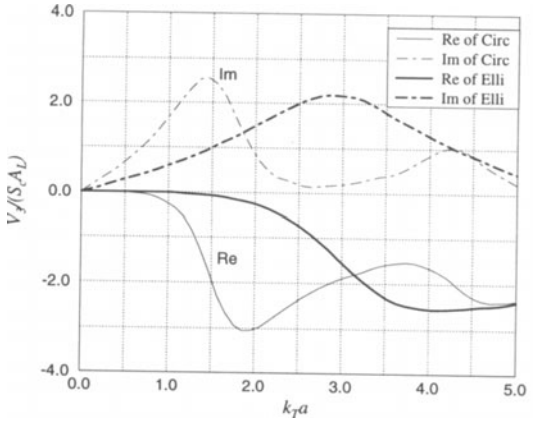

Figure 5. Normalized crack opening volume (V_3/S_cA_L) as a function of dimensionless wave number (k_Ta) for circular and elliptic cracks.

In Ref.[9] V_3 has been calculated with the boundary integral equation method. The normalized crack opening volume $V_3/(S_cA_L)$ calculated in Ref.[9] has been plotted against the dimensionless wave number k_Ta in Fig. 5. It has a real part and a imaginary part. The thin lines are for the crack opening volume of a circular crack and the thick lines are for the crack opening volume of an elliptical crack. Note that for the higher frequencies ($k_T\lambda >> 1$), the values of the real parts appear to oscillate about -2, which agrees with the Kirchhoff approximation.

Once the scattering coefficient has been obtained, we can calculate the scattered displacement field with the following expression

$$u_f(x_i^2,t) = FFT^{-1}\{FFT[u_f(x_i^1,t)]S_{21}(\omega)\} \tag{12}$$

where $u_f(x_i^1,t)$ is the displacement field transmitted by transducer 1 and $u_f(x_i^2,t)$ is the displacement field received by transducer 2 after the scattering by the crack.

SIMULATION OF SELF-FOCUSING OF AN ARRAY

The configuration for the simulation is shown in Fig. 6. The array consists of eleven transducers. It is circularly pre-focused with a radius of curvature of 330 mm. The array transducer is in circular shape and the diameter is 5 mm. The natural focal

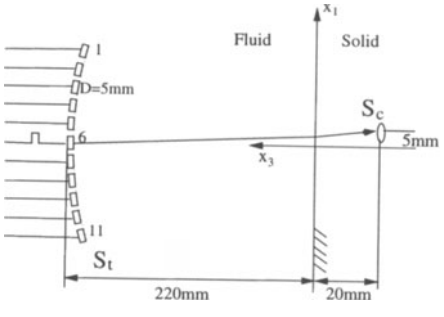

Figure 6. A system for detecting an interior crack.

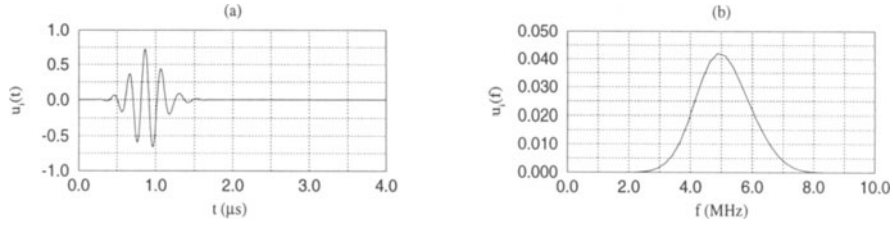

Figure 7. Signal generated by single element transducer (a) in time domain (b) in frequency domain.

point is located on the axis and behind the crack. The signal generated by a single element is shown in Fig. 7. The center frequency of the single element transducer is 5 MHz with a band width of about 2 MHz at 6dB attenuation. In the following numerical calculations, 80dB amplification has been applied to the scattered displacement signals.

The numerical simulations have been performed for various configurations as shown in Fig. 8. The first case shown in Fig. 8(a,b) is for a circular crack with radius equal to 0.2mm. The signals are transmitted out with appropriate time delays to achieve the sonification focusing and reception focusing is used to sum up the received signals. The total signal is clean with a big amplitude.

The second case shown in Fig. 8(c,d) is for the same configuration and crack size, but without applying self-focusing. The signals are sent out at the same time and the received amplitudes are summed up without reception focusing. The total displacement signal is not as nice and the amplitude is much smaller compared with the one calculated for self-focusing. The advantage of the self-focusing can be seen by comparing Fig. 8(a) with Fig. 8(c) and Fig. 8(b) with Fig. 8(d).

The third case shown in Fig. 8(e,f) is for a circular crack with a smaller radius (0.1mm). The self-focusing procedure has been performed. For the smaller crack, the same incident field will cause a smaller crack opening volume. Therefore, the scattering coefficient will be much smaller. The displacement amplitude is about one ninth of the one shown in Fig. 8(a).

The last case shown in Fig. 8(g,h) is for an elliptical crack with the long axis equal to 0.2mm and the short axis is 1/3 of the long axis. The self-focusing procedure has been performed. The crack opening volume of the elliptical crack is small and the final displacement signal is small as compared with the one for the circular crack of the first case. We also note from the plots in the frequency domain shown in Fig. 8(f,h), that the small crack and the elliptical crack scatter more high frequency components as compared with the bigger circular crack.

CONCLUSIONS

Self-focusing of an array on an interior crack has been simulated. The transducer field has been represented by a Gaussian distribution and ray tracing has been used to obtain the incident wave field on the crack inside an immersed specimen. A reciprocity relation has been employed to calculate the scattering coefficient of the crack. Self-focusing produces a much better signal of much larger amplitude. Numerical modeling of the self-focusing process can serve as a flexible tool for examining the effects of experimental parameters.

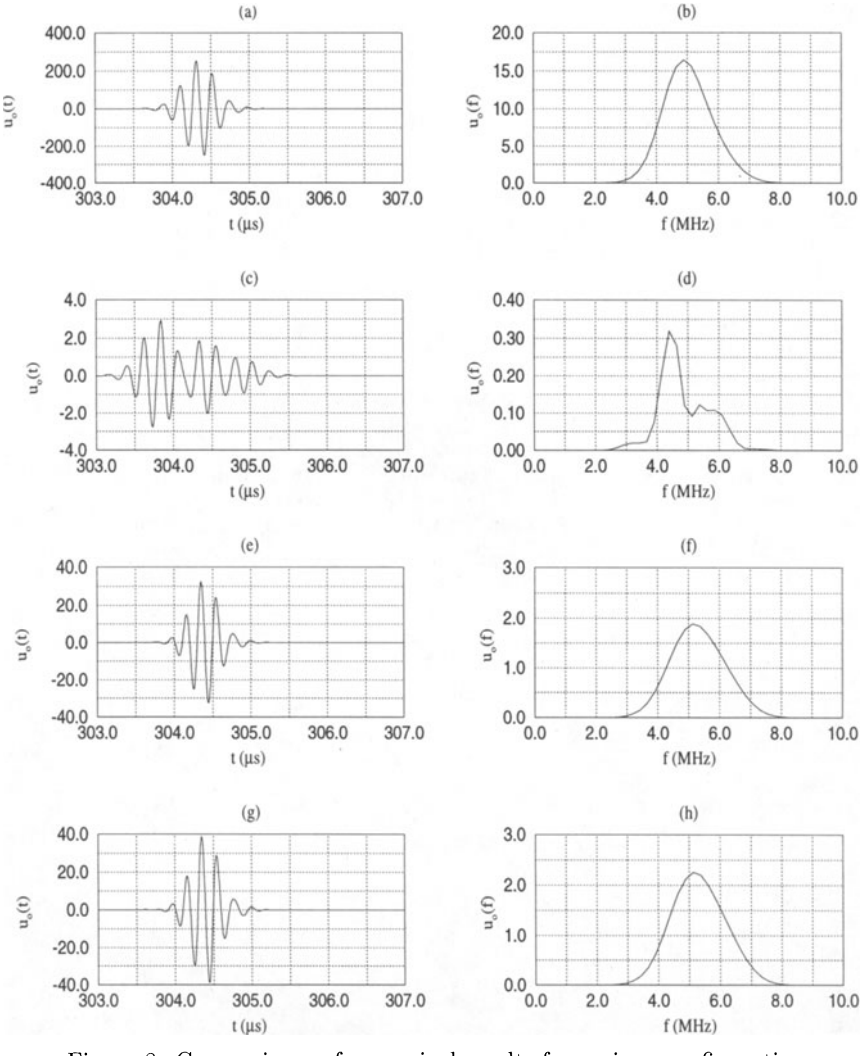

Figure 8. Comparisons of numerical results for various configurations.

ACKNOWLEDGMENT

This work was carried out in the course of research funded by the AFOSR under Grant F49620-93-1-0257 and by the FAA under its Aging Aircraft Program at the Center for Aviation Systems Reliability (CASR).

REFERENCES

1. N. Chakroun, M. Fink and F. Wu, Time Reversal Processing in Ultrasonic Nondestructive Testing, *IEEE Trans. Ultrason. Ferroelec. Freq. Contr.* 42:1087-1097 (1995)
2. B. Beardsley, M. Peterson and J. D. Achenbach, A Simple Scheme for Self-Focusing of an Array, *J. NDE,* Vol. 14, No. 4:169-179 1995
3. O. T. von Ramm and S. W. Smith, Beam Steering with Linear Arrays, *IEEE Trans. Biomed. Eng.* 30:438-452 (1983).
4. D. H. Turnbull and F. S. Foster, Beam Steering with Pulsed Two-dimensional Transducer Arrays, *IEEE Trans. Ultrason. Ferroelec. Freq. Contr.* 38:320-333 (1991)
5. J. Krautkrämer, H. Krautkrämer, Ultrasonic Testing of Materials, 4th ed. Springer-Verlag, 1990
6. B. A. Auld, General Electromechanical Reciprocity Theory Relations Applied to the Calculation of Elastic Wave Scattering Coefficients, *Wave Motion* 1:3-15 (1979)
7. G. S. Kino, The Application of Reciprocity Theory to Scattering of Acoustic Waves by Flaws, *J. Appl. Phys.* 49(6):3190-3199 (1978)
8. R. B. Thompson and T. A. Gray, A Model Relating Ultrasonic Scattering Measurements Through Liquid-Solid Interfaces to Unbounded Medium Scattering Amplitudes, *J. Acoust. Soc. Am.* 74(4):1279-1290 (1983)
9. D. E. Budreck and J. D. Achenbach, Scattering From Three Dimensional Planar Cracks by the Boundary Integral Equation Method, *J. Appl. Mech.* 55:405-412 (1988)